

Seismic mitigation of an existing building by connecting to a base-isolated building with visco-elastic dampers

Zhidong Yang* and Eddie S.S. Lam

Department of Civil & Environmental Engineering, The Hong Kong Polytechnic University, Hong Kong

(Received April 29, 2013, Revised May 1, 2014, Accepted June 19, 2014)

Abstract. This study investigates the feasibility of retrofitting an existing building by connecting the existing building to a new building using connecting dampers. The new building is base-isolated and visco-elastic dampers are assigned as connecting dampers. Scaled models are tested under three different earthquake records using a shaking table. The existing building and the new building are 9 and 8 stories respectively. The existing building model shows more than 3% increase in damping ratio. The maximum dynamic responses and the root mean square responses of the existing building model to earthquakes are substantially reduced by at least 20% and 59% respectively. Further, numerical models are developed by conducting time-history analysis to predict the performance of the proposed seismic mitigation system. The predictions agree well with the test results. Numerical simulations are carried out to optimize the properties of connecting dampers and base isolators. It is demonstrated that more than 50% of the peak responses can be reduced by properly adjusting the properties of connecting dampers and base isolators.

Keywords: experimental study, base isolation, connecting damper, adjacent buildings, seismic mitigation

1. Introduction

Recently, an innovative strategy has been studied to reduce the responses of adjacent buildings to earthquake by connecting the buildings using dampers. For example, fluid dampers are used to link two adjacent buildings. Responses at different stiffness ratios and mass ratios are investigated (Xu *et al.* 1999a, Xu *et al.* 1999b). It has been demonstrated that responses of structures can be reduced by linking them with visco-elastic dampers (Kim *et al.* 2006) or friction dampers (Bhaskararao and Jangid 2006). Besides passive dampers, active dampers and semi-active dampers have also been studied (Seto *et al.* 1995, Christenson *et al.* 2007). It is well demonstrated that, with properly designed connecting dampers, responses of adjacent buildings to earthquake excitation can be mitigated. Further, efficiency of the above-mentioned structural system is affected by the ratio of lateral stiffness of adjacent buildings. In general, high ratio of lateral stiffness is preferred (Matsagar and Jangid 2005, Kim *et al.* 2006). To increase the ratio of lateral stiffness, a five-story fixed-base building is proposed to be connected to a four-story base-isolated building (Matsagar and Jangid 2005). As a result, seismic performance of the fixed-base building is improved (Matsagar and Jangid 2005). Also, response of a fixed-base building coupled to a base

*Corresponding author, Ph.D. Student, E-mail: 09902640r@connect.polyu.hk

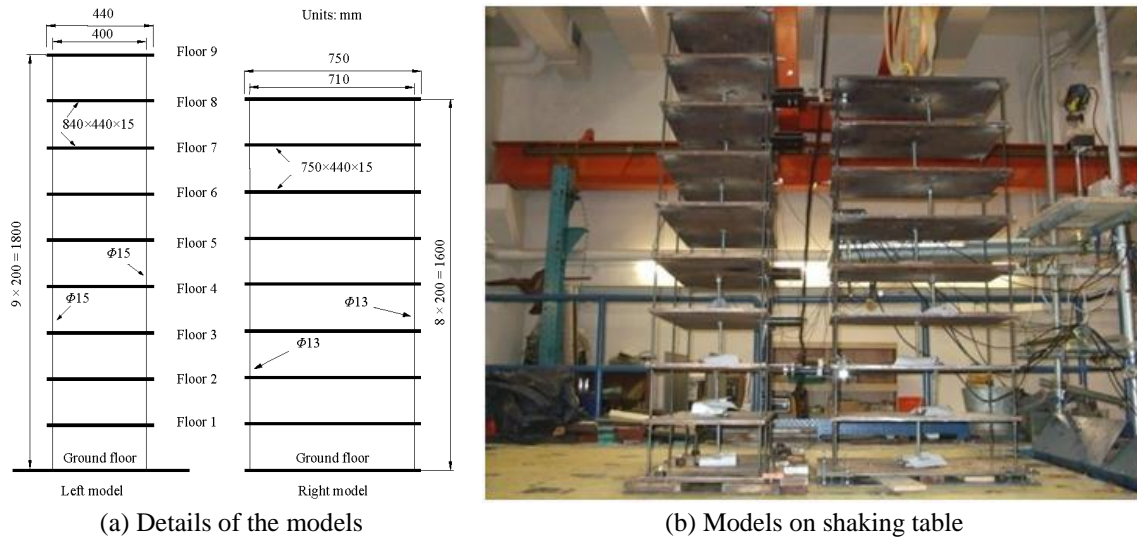


Fig. 1 Experimental models

isolated building by viscous dampers can be reduced (Matsagar and Jangid 2006).

The above is based on numerical simulations and it is desirable to perform an experimental investigation. For example, according to numerical simulations, seismic response of adjacent buildings can be reduced when connected together by friction dampers (Bhaskararao and Jangid 2006). However, experimental studies have shown that the maximum response of adjacent buildings connected by friction dampers may not be reduce as considered (Ng and Xu 2006, Xu and Ng 2008). Similar phenomena have also been observed when other types of dampers are used, e.g., magnetorheological dampers (Xu *et al.* 2005), active control actuators (Christenson *et al.* 2003).

Therefore, experimental studies are carried out in this study to explore the feasibility of mitigating the seismic responses of an existing building by connecting to a new building using visco-elastic dampers. The new building is base-isolated to provide large ratio of lateral stiffness between the new building and the existing building. Further, parametric studies are performed using numerical models to explore the effect of base isolators and the influence of changing the properties of connecting dampers to the response.

2. Building models

The existing building is a 9-story frame structure with fundamental period being at 0.94s. The new building has 8 stories. It has a fundamental period at 0.75 s with fixed base. The two buildings are scaled with a geometry ratio of 1/15. Considering the difficulties in full compliance with the simulation law, mass ratio and time ratio are assigned to be 1/27100 and 3/10, respectively. Such an approach has been successfully applied by previous researchers (Xu *et al.* 2005, Li *et al.* 2006, Roh *et al.* 2011).

The two models are shown in Fig. 1. On the left is the model representing the existing building (“the left model”). It is 1.8 m height and has a mass of 442.6 kg. 840 mm×440 mm×16 mm steel

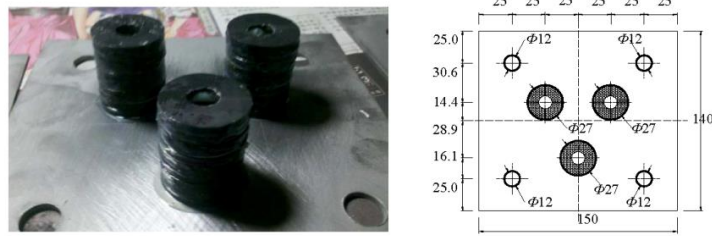


Fig. 2 Base isolators (measurement in mm)

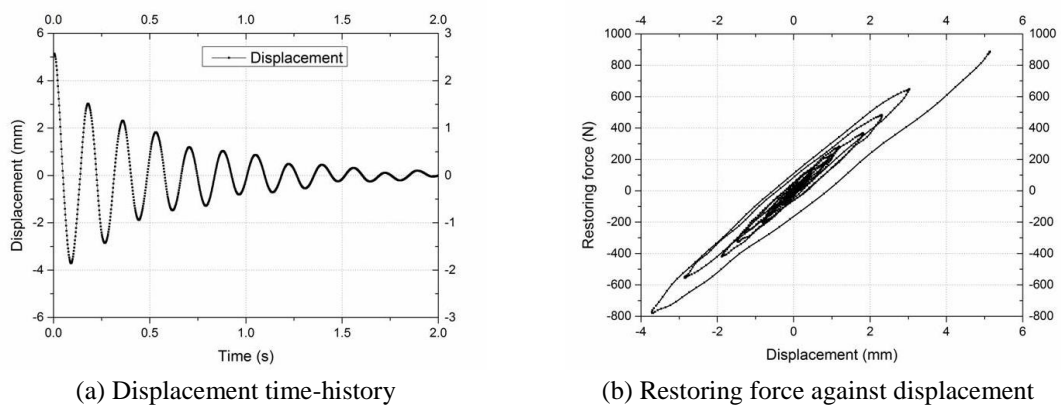


Fig. 3 Free vibration of the steel plates over base isolator

plates and 13 mm diameter steel bars are used to represent the floor slabs and columns respectively. On the right is the model for the new building (“the right model”) with a height of 1.6 m and a total mass of 364.7kg. 750 mm×440 mm×15 mm steel plates and 11 mm diameter steel bars are used to simulate floor slabs and columns respectively.

Ambient responses of the two models were measured by accelerometers installed at every floor. Applying Frequency Domain Decomposition Method (Brincker *et al.* 2001, Lamarche *et al.* 2008), natural frequencies and damping ratios of the models are estimated as shown in Table 5.

3. Base isolation system

The base isolators were specifically fabricated as shown in Fig. 2. Each base isolator comprises 3 columns of rubber bearings pressed between two steel plates. Each rubber bearing is consisted of 9 layers of cylindrical polyurethane pieces providing small lateral stiffness and 8 layers of steel washers to enhance its bearing capacity. Outer diameter, inner diameter and thickness of cylindrical polyurethane pieces are 27 mm, 10 mm and 3 mm, respectively. The steel washers have an outer diameter of 25 mm, an inner diameter of 10 mm and a thickness of 0.2 mm. Cylindrical polyurethane pieces and steel washers are glued together by epoxy. Averaged thickness of each rubber bearing is 32 mm.

4 isolators were tested on a shaking table. They were installed between two steel plates and the upper steel plate was loaded with a 360 kg mass. Accelerations under free vibration were

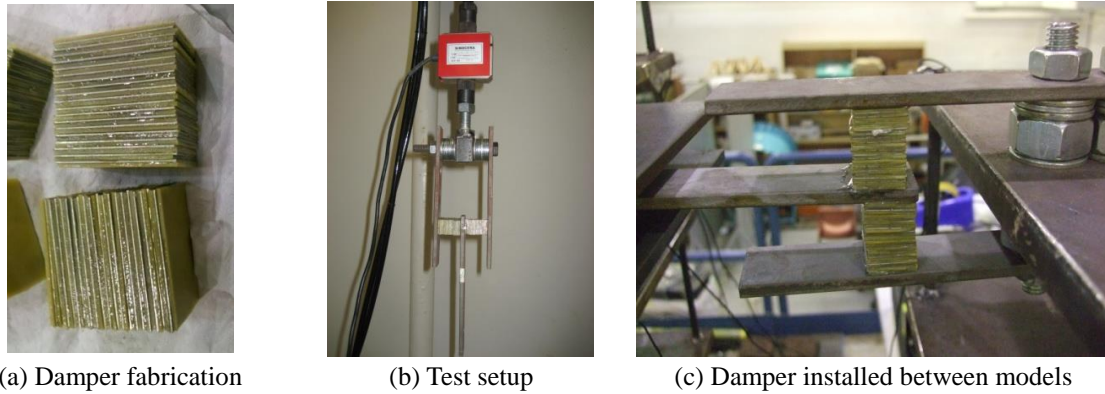


Fig. 4 Connecting dampers

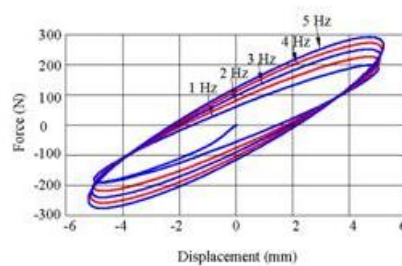


Fig. 5 Force-displacement relation of connecting dampers at 5mm displacement

measured. Fig. 3 presents plots of displacement against time and restoring force against displacement of the isolators. Equivalent lateral stiffness and equivalent damping ratio of the isolators are estimated to be $k_{iso} = 179.2\text{kN/m}$ and $\zeta_{iso} = 4.0\%$ respectively.

4. Connecting dampers

Connecting dampers comprise 20 layers of visco-elastic damping pads sandwiched by 19 layers of steel pads as shown in Fig. 4(a). Dimensions of visco-elastic damping pads and steel pads are $20\text{ mm} \times 30\text{ mm} \times 0.8\text{ mm}$. Height of a connecting damper is 16 mm.

4.1 Properties of connecting dampers

Properties of connecting dampers (visco-elastic dampers) were assessed by a MTS testing machine as shown in Fig. 4(b). Applied load was measured by a small capacity load cell. Sinusoidal actions at different frequencies (1 Hz to 5 Hz) and different amplitudes (1 mm to 5 mm) were applied. Connecting dampers performed well at different excitation frequencies and different displacement amplitudes. Fig. 5 gives the force-displacement relationships at 5mm displacement amplitude and different frequencies. Fig. 6 shows hysteresis loops of sinusoidal test at 5 Hz excitation and different displacement amplitudes. The two dashed lines as shown in Fig. 6 represent equivalent stiffness of dampers when the displacement amplitudes are 1 mm and 5 mm.

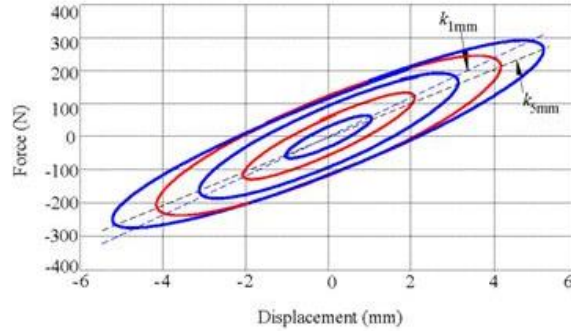


Fig. 6 Force-displacement relation of connecting dampers at different amplitudes at 5Hz

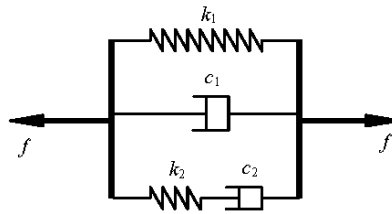


Fig. 7 Connecting damper model

4.2 Connecting damper model

Various models have been applied to simulate the behaviour of connecting dampers. Kelvin model and Maxwell model connected in parallel as shown in Fig. 7 (a special kind of general mechanical model) provide the best representation of connecting dampers at frequencies between 1 Hz and 5 Hz. Total damper force is expressed by the following equation

$$f = f_k + f_m \tag{1}$$

where f_k and f_m are the forces in the Kelvin component and the Maxwell component respectively. $f_k = k_1\Delta + c_1\dot{\Delta}$, and $\dot{f}_m/k_2 + f_m/c_2 = \dot{\Delta}$ (Constantinou *et al.* 1998). Δ and $\dot{\Delta}$ are the respective relative displacement and relative velocity between the two ends of connecting dampers.

As shown in Fig. 7 and Table 1, the connecting damper model is defined by four parameters k_1, c_1, k_2 and c_2 . The parameters are computed by performing regression analysis on the aforementioned test data. The stiffness of the connecting damper model changes with the variation of the displacement amplitude as shown in Fig. 8. To explore the relationship between the stiffness and the displacement amplitude, non-linear curve fitting has been done. It is found that the following function can be used to predict the stiffness k_1 and k_2

$$k_i = \frac{\Delta a^2 b}{\Delta^2 b_2 + a^2} + k_0 \tag{2}$$

where $i=1,2$. Constants a, b and k_0 are given in Table 2.

Table 1 Properties of connecting dampers

Amplitude (mm)	Stiffness k_1 (kN/m)	Damping c_1 (Ns/m)	Stiffness k_2 (kN/m)	Damping c_2 (Ns/m)	Correlation coefficient
1	38.205	663.7	20.055	1166.8	0.9998
2	38.682	663.7	20.984	1166.8	0.9992
3	36.244	663.7	18.809	1166.8	0.9998
4	34.601	663.7	16.364	1166.8	0.9996
5	33.831	663.7	14.589	1166.8	0.9991

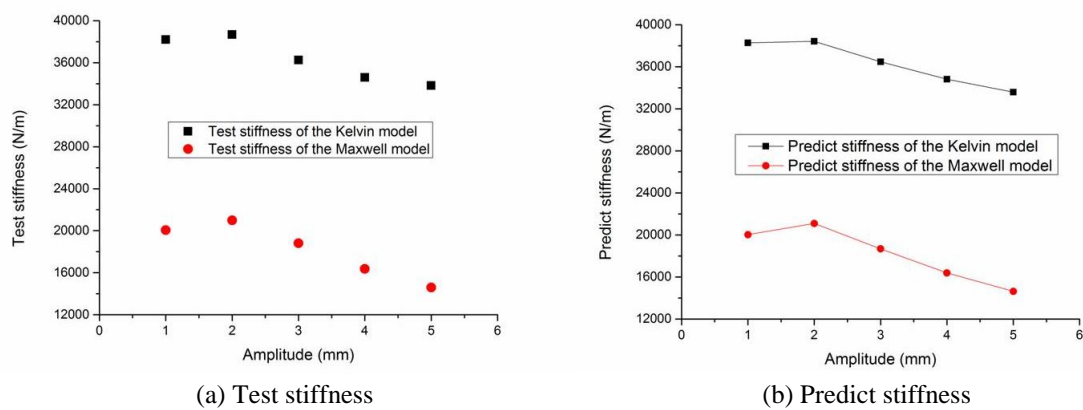


Fig. 8 Stiffness of the connecting damper model against amplitude

Table 2 Properties of connecting dampers

Stiffness	a (kN/m)	b (MN/m)	k_0 (kN/m)	Coefficient of correlation
k_1	23.269	16.129	27.383	0.9937
k_2	32.326	20.573	5.384	0.9994

Table 3 Predicted stiffness of connecting dampers at different displacement amplitudes

Amplitude (mm)	Stiffness k_1 (kN/m)	Error (%)	Stiffness k_2 (kN/m)	Error (%)
1	38.278	0.19	20.026	-0.14
2	38.424	-0.67	21.088	0.50
3	36.472	0.63	18.671	-0.73
4	34.810	0.60	16.385	0.13
5	33.581	-0.74	14.630	0.28

Errors between predicted values and the test data are shown in Table 3. The maximum differences for k_1 and k_2 are 0.74% and 0.73% respectively.

5. Shaking table test

5.1 Test arrangement

The two models were tested on a shaking table. The test can be divided into three stages.

(1) At stage one, both models were bolted to the shaking table and subjected to random vibration using a hammer to estimate frequencies and damping ratios.

(2) At stage two, three earthquake records as shown in Table 4 (GB50011-2010 2010) were used to excite the models.

(3) At stage three, base isolators were installed to the right model and connecting dampers were incorporated between the models as shown in Fig. 1. Connecting dampers were installed at the 8th floor where the maximum response occurs and at the 2nd floor to reduce displacement of the right model. The coupled seismic mitigation system was subjected to three earthquake records as shown in Table 4 (GB50011-2010 2010). The three earthquake records are scaled with peak accelerations being at 1m/s² and time intervals reduced to 0.3 of the original data.

5.2 Test results

Based on the acceleration records obtained at stage one, fundamental frequencies f and damping ratios ζ are estimated. The results are given in Table 5. In the table, “Separated” and “Coupled” represent two different cases, with the left model and the right model separated and coupled by connecting dampers respectively. Fundamental frequencies are reduced when connecting dampers are installed. Especially, fundamental frequencies of the right model are shifted by around 30%. Damping ratios for the first two modes of both models have significantly increased.

Fig. 9 compares displacement at top floor level of the left model when subjected to Hachinohe earthquake. Two cases are presented, namely with and without connecting dampers. Response of the left model is significantly reduced in the presence of connecting dampers. Similar responses are observed when the models are subjected to the other two earthquake records.

Table 6 compares amplification factors of the left model under different earthquake records. Amplification factor of the root-mean-squares acceleration at floor k is estimated in the form of

$$r_{\text{RMS}} = \frac{1}{a_{\text{max, st}}} \sqrt{\frac{1}{N} \sum_{i=1}^N \ddot{x}_{i,k}^2} \quad (3)$$

Table 4 Earthquake records

Earthquake	Station	Component	Year	Characteristic frequency
Tokachi-Oki	Hachinohe harbor	West-east	1968	4.17 Hz~25 Hz
Imperial Valley	EI Centro	Impvalli-Elc180	1940	6.25 Hz~25 Hz
Kobe	Takarazuka	TAZ090	1995	4.17 Hz~25 Hz

Table 5 Modal frequencies and damping ratios of the models

Mode	Left Model				Right model			
	Separated		Coupled		Separated (fixed base)		Coupled	
	f (Hz)	ζ (%)	f (Hz)	ζ (%)	f (Hz)	ζ (%)	f (Hz)	ζ (%)
1st	3.78	0.64	3.37	4.22	4.81	0.47	3.40	4.22
2nd	11.44	0.44	11.70	4.32	14.77	0.60	10.35	4.70

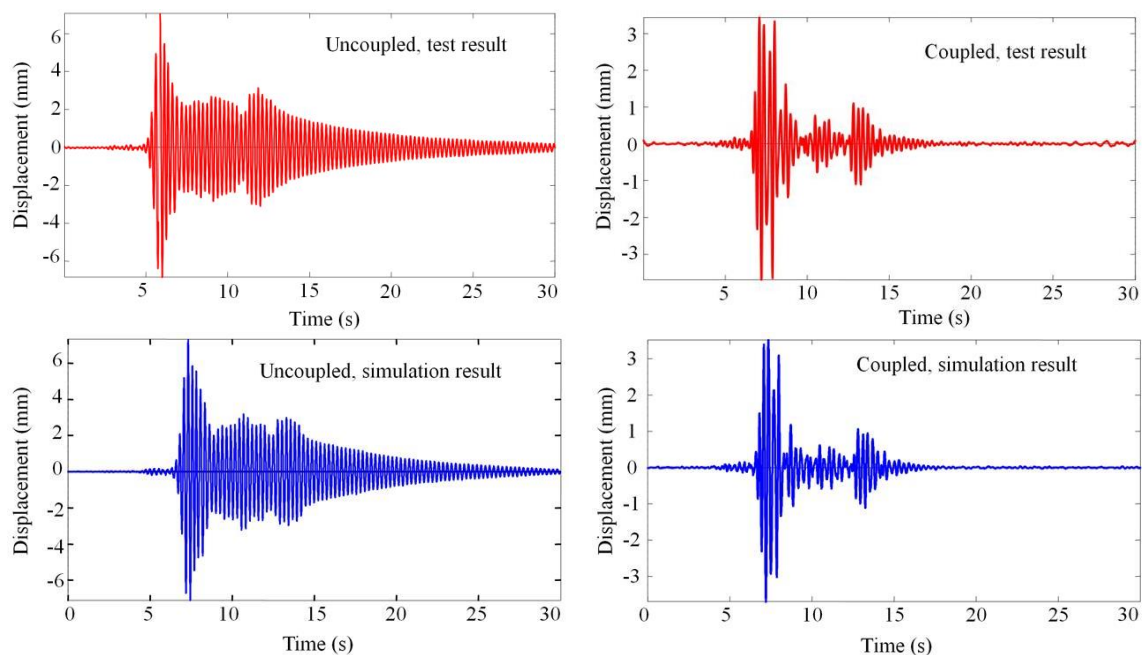


Fig. 9 Top floor displacement of the left model under Hachinohe earthquake

Table 6 Comparison of amplification factors of the left model

Earthquake	Response	Uncoupled	Coupled	Percentage reduction (%)
Hachinohe	Peak acceleration	4.71	2.81	40.28
	Peak displacement	6.58	3.99	39.33
El Centro	Peak acceleration	3.45	2.58	25.29
	Peak displacement	5.77	4.61	20.06
Kobe	Peak acceleration	5.50	2.96	46.16
	Peak displacement	8.72	4.95	43.17
Hachinohe	RMS acceleration	1.15	0.45	60.92
	RMS displacement	1.86	0.76	59.35
El Centro	RMS acceleration	1.02	0.37	64.10
	RMS displacement	1.71	0.69	59.91
Kobe	RMS acceleration	1.50	0.52	65.27
	RMS displacement	2.56	1.02	60.18

where $a_{\max, st}$ is the maximum acceleration of the shaking table. N is the total number of test data. Sampling rate and duration of the shaking table tests are 1000Hz and 30s, respectively, i.e., $N=3 \times 10^4$. $\ddot{x}_{t_i, k}$ is the acceleration response at floor k at instant t_i . Similarly, amplification factor of the RMS displacement response can also be obtained.

The maximum accelerations and the maximum displacements of the left model are reduced by at least 20% and RMS values are decreased by more than 60%. This indicates that the left model (representing an existing building) can be effectively protected when connected to the new building using connecting dampers.

Table 7 Comparison of amplification factors of the right model

Response	Earthquake	(A) Uncoupled (fixed base)	(B) Uncoupled (base-isolated)	(C) Coupled	$\frac{(A) - (B)}{(A)} \times 100\%$
Peak acceleration	Hachinohe	5.28	1.91	2.54	51.98
	El Centro	4.44	1.66	2.16	51.48
	Kobe	6.90	1.82	3.11	55.00
RMS acceleration	Hachinohe	1.45	0.26	0.52	63.86
	El Centro	1.43	0.27	0.40	72.16
	Kobe	2.39	0.25	0.64	73.30
Peak displacement	Hachinohe	4.73	3.41	4.55	3.81
	El Centro	4.34	5.64	5.82	-34.10
	Kobe	8.04	6.08	7.42	7.71
RMS displacement	Hachinohe	0.65	0.61	0.62	4.62
	El Centro	0.42	0.82	0.70	-66.67
	Kobe	0.73	0.72	0.79	-8.22

Table 7 compares responses of the right model to three earthquake records. By connecting the isolated right model and the left model, acceleration response of the isolated right model is adversely increased. However, peak acceleration and RMS acceleration of the right model in the proposed seismic mitigation system are still relatively small and more than 51% and 63% reductions have been achieved respectively. Peak displacements of the right model as given in Table 7 include displacement of base isolators and the right model. Around 55%, 41% and 51% of peak displacements of the right model are contributed by the base isolators under the respective earthquake record.

6. Analytical study

To complete the investigation on the effectiveness of using connecting dampers, parametric studies are performed. An analytical model is developed using a two-dimensional shear model.

6.1 Equations of motion and simulation results

Equations of motion are based on a two-dimensional formulation in the form of (Humar 2012)

$$[M][\ddot{X}] + [C][\dot{X}] + [K][X] + [R]_d = -[M][I][\ddot{X}]_s \quad (4)$$

where $[R]_d$ is a vector representing the nonlinear forces of the connecting dampers and can be calculated by Eq. (1) and Eq. (2). $[X]$, $[\dot{X}]$ and $[\ddot{X}]$ are respective the displacement vector, velocity vector and acceleration vector relative to the ground. $[\ddot{X}]_s$ is the shaking table acceleration vector. $[I]$ is a unit vector.

The mass matrix $[M]$ is

$$[M] = \begin{bmatrix} [M]_l \\ [M]_r \end{bmatrix} \quad (5)$$

Table 8 Masses and stiffness at each floor level

	Left model		Right model	
	Mass (Kg)	Stiffness (kN/m)	Mass (Kg)	Stiffness (kN/m)
Base floor	44.3	965.21	36.5	179.20
Other floor	44.3	965.21	41.2	1105.17

where $[M]_l$ and $[M]_r$ are respective the mass matrix of the left model and mass matrix of the right model. Subscripts l and r represent the left model and the right model, respectively. In this study, masses are lumped at each floor level as shown in Table 8.

The stiffness matrix $[K]$ is

$$[K] = \begin{bmatrix} [K]_l & \\ & [K]_r \end{bmatrix} \quad (6)$$

where $[K]_l$ and $[K]_r$ are respective the stiffness matrix of the left model and the right model. The damping matrix $[C]$ is similar to the stiffness matrix $[K]$. For the left model, Rayleigh damping is assumed using damping ratios of the first and second modes (Table 5). For the right model, stiffness proportional damping is adopted at isolation layer (i.e., $2\zeta_{iso}k_{iso}/\omega_{r,1}$ in which $\omega_{r,1}$ is the 1st modal frequency of the right model).

A finite element model was developed using ANSYS to estimate lateral stiffness of the two models and the results are $k_1^0 = 874.5\text{kN/m}$ and $k_r^0 = 1092.2\text{kN/m}$. Using these values as the basis, lateral stiffness is updated based on the experiment data. As an example, the procedure for updating lateral stiffness of the left model is as shown in Fig.10. The updated lateral stiffness is given in Table 8. Since modal frequency identification is more accurate than mode shape or damping identification (Hemez and Doebling 2001), modal frequency is used to update the stiffness of the models. The objective function is

$$J(k) = \sum_{i=1}^n \alpha_i (f_{a,i} - f_{e,i})^2 \quad (7)$$

where $f_{a,i}$ and $f_{e,i}$ are the i th modal analytical and experimental frequencies, respectively and $n = 3$. α_i are weighting factors assigned arbitrary according to modal participation. α_1, α_2 and α_3 are 0.8, 0.15 and 0.05, respectively. As fundamental mode is the dominant mode, a larger value is assigned to α_1 .

Eq. (4) is rewritten in incremental form and is solved by the Newmark- β method in combination with the Newton-Raphson method to obtain the responses (e.g., acceleration, velocity and displacement) at any time t numerically (Datta 2010). Responses of the models to Hachinohe earthquake are illustrated in Fig. 9 and Fig. 11. Simulated displacements at top floor of the models agree well with corresponding test data (Fig. 9 and Fig. 11). This indicates that the analytical model is accurate.

6.2 Parameter studies

Effectiveness of connecting dampers is affected by many factors including shear area of connecting dampers, stiffness of the base isolators and damping ratio of the base isolators. To

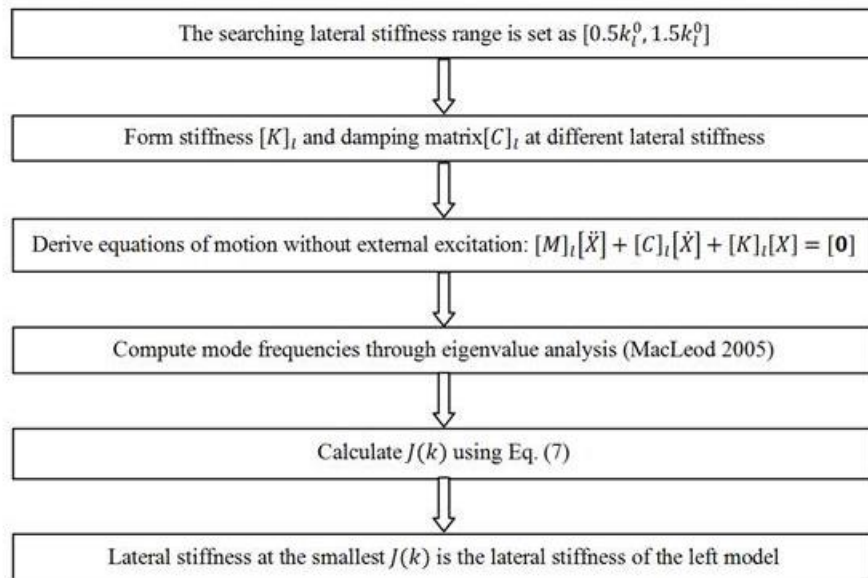


Fig. 10 Procedure to determine the lateral stiffness of the left model

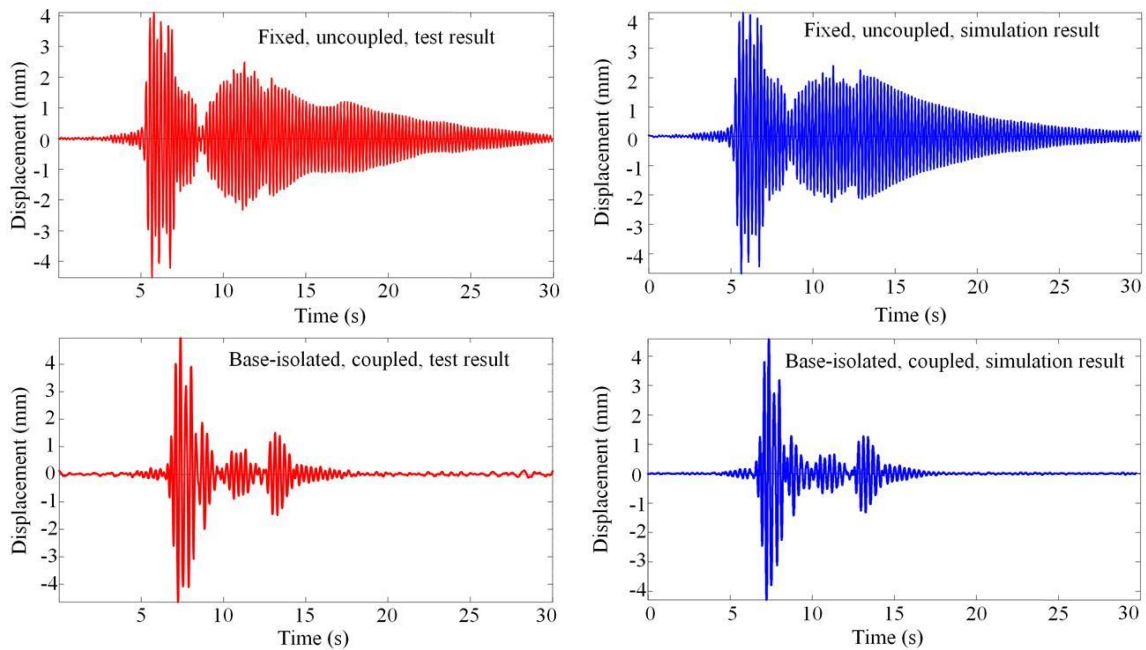


Fig. 11 Test and simulation displacement of top floor of the right model under Hachinohe

investigate the effect of these factors on the performance of the proposed seismic mitigation system, extensive analytical studies have been carried out to compute the maximum responses of the left model at different damper sizes, different total base isolator stiffness and different damping. The parameters to be considered include shear area of connecting damper from 0 mm² to

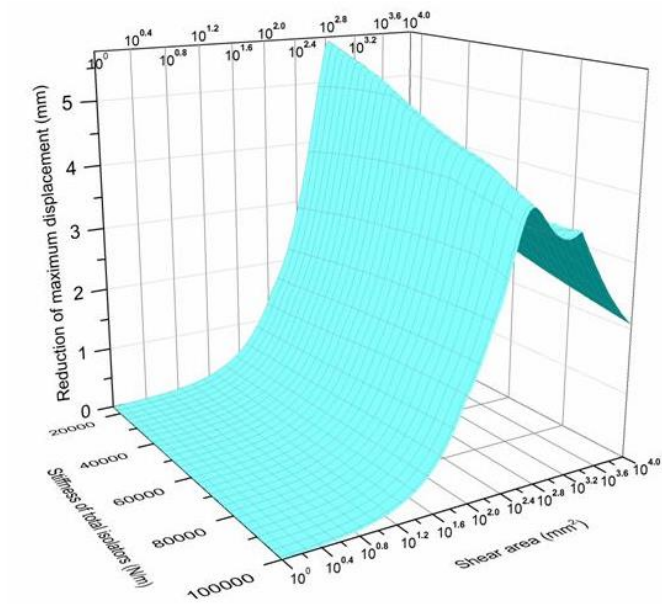


Fig. 12 Reduction of the maximum displacement of the left model against connecting damper area

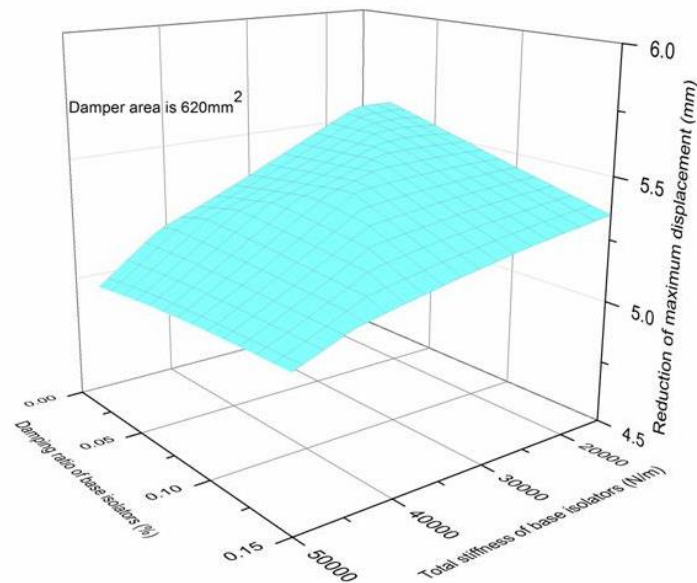


Fig. 13 Reduction of maximum displacement of the left model against total stiffness

$1 \times 10^4 \text{ mm}^2$, damping ratio of base isolators from 3% to 15% and stiffness of base isolators from 18.6 kN/m to 44.4 kN/m (so that fundamental period of corresponding base-isolated building is between 2 and 3s).

When the coupled models are excited by Hachinohe earthquake, reduction of the maximum displacement of the left model against different shear areas at different total stiffness of base

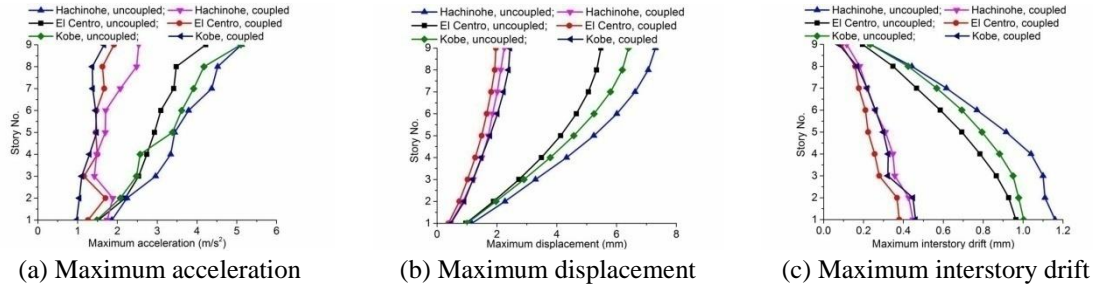


Fig. 14 Comparison of peak response envelopes of the left model

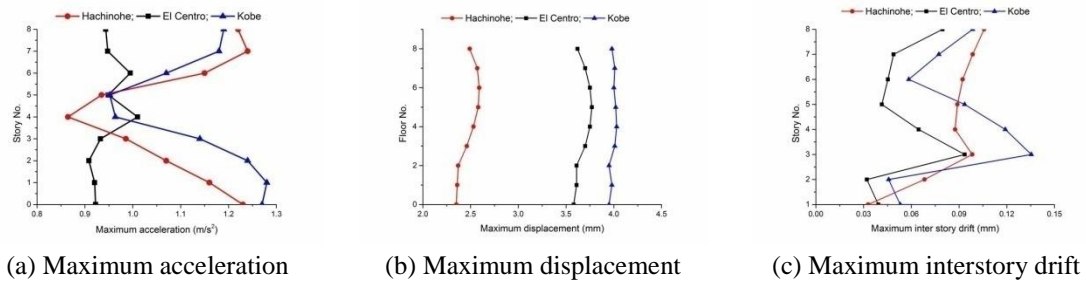


Fig. 15 Peak response envelopes of the right model

isolators is illustrated in Fig. 12. Critical shear area of connecting damper is $A_{Hachinohe} = 620 \text{ mm}^2$.

When shear area is 620 mm^2 , influence of total stiffness of base isolators to maximum displacement response of the left model (to Hachinohe earthquake) at various damping ratios of base isolators is shown in Fig. 13. Total stiffness of base isolators of the right model has significantly affected the responses of the left model. Increasing total stiffness of the base isolators reduces the maximum displacement of the left model. This favours the use of smaller total stiffness. Within the range from 18.64 kN/m to 44.4 kN/m , the preferred total stiffness is 18.6 kN/m .

When the shear area is 620 mm^2 , the variation of the maximum response due to change in damping ratio of the base isolators is less than 10%. Hence, damping ratio of the base isolators is not a dominant factor that significantly affects the responses of the seismic mitigation system. In this study, damping ratio of the base isolators is selected as 4.0%.

Similarly, critical shear are as $A_{El\ Centro}$ for El Centro earthquake and A_{Kobe} for Kobe earthquake are estimated to be 450 mm^2 and 400 mm^2 respectively. Considering the range of the damper area is between 400 mm^2 and 620 mm^2 , an average damper area (i.e. $(A_{Hachinohe} + A_{El,Centro} + A_{Kobe})/3 = 490 \text{ mm}^2$) is used in the following section.

6.3 Comparison of response

Fig. 14 shows the response envelopes of the left model to the three earthquake records with shear area of connecting dampers at 490 mm^2 , total stiffness of base isolators of the right model at 18.6 kN/m and damping ratio of base isolators at 4.0%. In comparison with the responses of the left model without connecting damper, the maximum acceleration responses, the maximum

displacement responses and the maximum drift responses to the three earthquakes are reduced by more than 50%, 61% and 50.6%, respectively. The reductions indicate that connecting dampers are effective in mitigating the responses of the left model.

Fig. 15 shows the response envelopes of the right model. Peak acceleration is less than 1.27m/s^2 and peak inter-story drift is less than $1/1450$. In fact, more than 90% of the maximum horizontal displacement occurs at isolation layer.

7. Conclusions

In this study, a seismic mitigation system using connecting dampers to connect an existing building to a base-isolated building is investigated. Visco-elastic dampers are assigned as connecting dampers. Scaled models were constructed and tested on a shaking table to investigate the feasibility of the proposed seismic mitigation system.

Experimental results have shown that damping ratios of the existing building have increased by more than 3%. The maximum dynamic responses and RMS responses to earthquake records are mitigated by at least 20% and 59%, respectively.

Further, numerical models were developed to perform time history analysis to predict the performance of the proposed seismic mitigation system. Numerical predictions agree well with the test results. This indicates that the analytical model is accurate. Extensive simulations are carried out to identify factors that significantly affect the proposed seismic mitigation system. It is demonstrated that shear properties of connecting dampers and total stiffness of base isolators are two dominant factors. More than 50% reduction on peak response can be achieved with proper selection of the properties of connecting dampers and base isolators.

References

- Bhaskararao, A. and Jangid, R. (2006), "Seismic analysis of structures connected with friction dampers", *Eng. Struct.*, **28**(5), 690-703.
- Brincker, R., Zhang, L. and Andersen, P. (2001), "Modal identification of output-only systems using frequency domain decomposition", *Smart Mater. Struct.*, **10**(3), 441.
- Christenson, R.E., Spencer Jr, B., Hori, N. and Seto, K. (2003), "Coupled building control using acceleration feedback", *Comput. Aid. Civil Inf.*, **18**(1), 4-18.
- Christenson, R.E., Spencer, Jr. B. and Johnson, E.A. (2007), "Semiactive connected control method for adjacent multidegree-of-freedom buildings", *J. Eng. Mech.*, **133**(3), 290-298.
- Constantinou, M.C., Soong, T.T. and Dargush, G.F. (1998), *Passive energy dissipation systems for structural design and retrofit*, Multidisciplinary Center for Earthquake Engineering Research Buffalo, NY
- Datta, T.K. (2010), *Seismic analysis of structures*, Wiley, Singapore.
- GB50011-2010 (2010), *Code for seismic design of buildings*, Chinese Architecture & Building Press, Beijing.
- Hemez, F.M. and Doebling, S.W. (2001), "Review and assessment of model updating for non-linear, transient dynamics", *Mech. Syst. Signal Pr.*, **15**(1), 45-74.
- Humar, J.L. (2012), *Dynamics of structures*, CRC Press LLC
- Kim, J., Ryu, J. and Chung, L. (2006), "Seismic performance of structures connected by viscoelastic dampers", *Eng. Struct.*, **28**(2), 183-195.
- Lamarche, C., Paultre, P., Proulx, J. and Mousseau, S. (2008), "Assessment of the frequency domain decomposition technique by forced-vibration tests of a full-scale structure", *Earthq. Eng. Struct. D.*,

- 37(3), 487-494.
- Li, C., Lam, S., Zhang, M. and Wong, Y. (2006), "Shaking table test of a 1: 20 scale high-rise building with a transfer plate system", *J. Struct. Eng.*, **132**(11), 1732-1744.
- MacLeod, I.A. (2005), *Modern Structural Analysis: Modelling Process and Guidance*, Thomas Telford, London.
- Matsagar, V.A. and Jangid, R. (2006), "Base-isolated building connected to adjacent building using viscous dampers", *Bull. New Zealand Soc. Earthq. Eng.*, **39**(1), 59-80.
- Matsagar, V.A. and Jangid, R.S. (2005), "Viscoelastic damper connected to adjacent structures involving seismic isolation", *J. Civil Eng. Manag.*, **11**(4), 309-322.
- Ng, C.-L. and Xu, Y.-L. (2006), "Seismic response control of a building complex utilizing passive friction damper: Experimental investigation", *Earthq. Eng. Struct. D.*, **35**(6), 657-677.
- Roh, H., Cimellaro, G.P. and Lopez-Garcia, D. (2011), "Seismic response of adjacent steel structures connected by passive device", *Adv. Struct. Eng.*, **14**(3), 499-517.
- Seto, M., Toba, Y. and Matsumoto, Y. (1995). "Reduced order modeling and vibration control methods for flexible structures arranged in parallel", *Proceedings of the American Control Conference*.
- Xu, Y.L., Chen, J., Ng, C. and Qu, W. (2005), "Semiactive seismic response control of buildings with podium structure", *J. Struct. Eng.*, **131**(6), 890-899.
- Xu, Y.L., He, Q. and Ko, J. (1999a), "Dynamic response of damper-connected adjacent buildings under earthquake excitation", *Eng. Struct.*, **21**(2), 135-148.
- Xu, Y.L. and Ng, C. (2008), "Seismic protection of a building complex using variable friction damper: experimental investigation", *J. Eng. Mech.*, **134**(8), 637-649.
- Xu, Y.L., Zhan, S., Ko, J. and Zhang, W. (1999b), "Experimental investigation of adjacent buildings connected by fluid damper", *Earthq. Eng. Struct. D.*, **28**(6), 609-631.